INSTRUMENTS FOR ADHESION AND FRICTION MEASUREMENTS AT MICRO/NANO SCALE

N.K. MYSHKIN, A.Ya. GRIGORIEV, A.M. DUBRAVIN, O.YU. KOMKOV and A.V. KOVALEV
Metal-Polymer Research Institute, Kirova st. 32A, 246050 Gomel, Belarus

SUMMARY

Development of miniature mechanical systems brings attention of many researchers to friction, lubrication, and wear problems in such systems. There is a scale factor affecting the data for macroscopic and nano/micro systems, so the test equipment should be designed with account of this factor. We describe such equipment including adhesion meter, rotary and reciprocating microtribometers. The adhesion meter allows us to measure force-distance dependence between the test samples in the nanometer range. The tribometers operate in the range of normal load from 0.01mN to 1N, velocity – from 0.1 to 10 mm/s and allow us to measure friction force and acoustic emission. We investigated adhesion forces between the ball probes and materials used in microsystems: silicon plates, steel plates, thin coatings, and self-assembled monolayers on silicon plates. Silicon, quartz and steel balls were used as probing samples. Friction tests were carried out using the same specimens as in adhesion tests. Advantages and drawbacks of instruments are discussed in relation to the scale and correlation of mechanical and physical factors affecting the contact interactions.

Keywords: Microtribology, adhesion, friction, testing equipment, self-assembled monolayers

1 INTRODUCTION

Modern high-technology systems operate in micro- and nanometer scale because their components are produced with very smooth surfaces [1].

Common macroscopic tribological principles cannot be applied directly to microsystems mainly due to influence of different factors on friction and wear in macro and microscale (Figure 1).

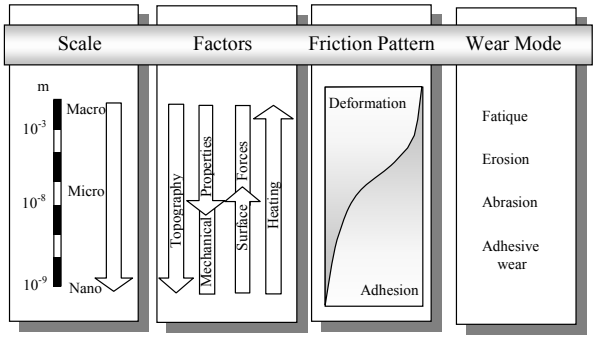

Figure 1: Combination of factors effecting friction and wear

Surface forces and adhesion are the dominant factors affecting the tribological behaviour at microscale. For example, it is known that operation of MEMS (micro-electro-mechanical systems) depends mainly on adhesion of parts in contact [2].

Much of research in microtribology is done with atomic force microscope (AFM), lateral force microscope (LFM), and surface force apparatus (SFA) [3, 4]. But these instruments provide data, which cannot be directly applied to real engineering systems. So, bridging the gap between macro and microtribology call for use the adequate test equipment.

We tried to design such equipment and apply to some objects offten used in microsystems.

2 EXPERIMENTAL EQUIPMENT

Usually the components of micro/nano systems operate under light loads (order of a few μN), that means in the range of values of surface forces. In order to simulate their operation efficiently we need to use the same range of loads as well as possibility to use combinations of contact geometry, materials and design of the test devices close to real applications.

2.1 Contact Adhesion Meter

The range of surface forces between the macroscopic bodies can be compared with the sensitivity of an accurate analytical balance. But the balance cannot be used to perform adhesion measurements because the surface forces increase rapidly with decreasing the distance between the test specimens. Hence, the measurements should be carried out at a very small speed impossible for common balance. Derjagin et al. proposed to solve the problem [5] by applying the principle of a feedback balance.

In our case we have chosen the design of a vertical torsion balance with negative feedback. This design eliminates the problems with balancing and errors caused by friction in the balance support.

The measuring unit of the contact adhesion meter (CAM) is a vertically disposed frame 1 (Figure 2) suspended on string 2. One arm of the frame carries holder 3 of a probing specimen (ball). Another arm of the frame carries movable coil 4 of a measuring electromagnet connected with a highly stable current source. Mirror 5 is fastened to the frame. It reflects the beam of laser 6, which then passes expander of optical base 7 and impinges photodetector 8. When force starts to act between the specimens frame 1 with mirror 5 turns thus changing the light flux impinging photodetector 8. The signal of the photodetector forms a feedback signal, which varies current in coil 9 until the frame has turned to its initial position. So, any variation in the forces acting between the specimens is compensated by a corresponding current variation that

remains the frame stationary in measuring process. Current in coil 9 is calibrated. So, the forces acting between specimen 10 and the ball can be measured.

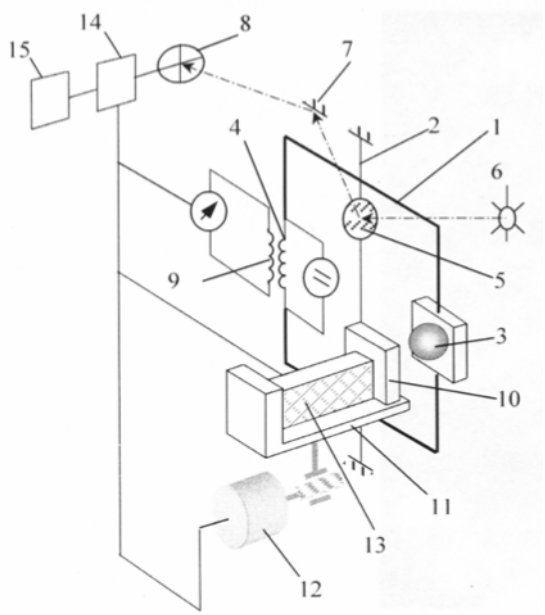

Figure 2: Principal scheme of adhesion meter

Specimen under testing 10 is placed on table 11 equipped with a system of rough positioning driven by stepping motor 12 and with a system of fine positioning driven by piezodrive 13.

Initially the specimen and the ball are removed to a distance at which they do not influence each other. Piezodrive 13 is stretched. In this position current passing measuring electromagnet 9 is assumed to correspond to zero force between the specimens. Then specimen 10 is approached to the probing specimen by stepping motor 12 until a preset initial contact load is attained. Depending on the aim of the experiment the measuring cycle can start either on reaching the required contact load or after a certain period of time.

Adhesion is measured when moving off specimen 10 with piezodrive 13 by plotting the dependence of the force acting between the specimens on the distance. In the process of moving off the force varies and this variation is compensated by current in coil 9 that provides a stationary position of the frame. When a preset distance is reached the measurement is performed in reverse order, namely when approaching the specimen to the probe. As a result, two dependencies are obtained characterizing the force of interaction when moving off and approaching the specimen to the ball.

To protect the apparatus from vibrations and to retain a constant temperature it was mounted on a table with a magnetic-fluid damper. The table is suspended on strings into a wooden case with a sound-proof lagging made of cellular polystyrene and metallized polyethylene film.

A programmable analog-digital signal processor 14 performs control of the measuring process.

The test data are processed and operation modes are set by software operating in Windows by the signal processor through a parallel port of PC 15. Basic characteristics of the apparatus are listed in the Table 1.

Measured forces, mN	0.01– 10
Sample displacements, nm	10 – 10000
Sample size, mm	20×20×5
Probe size (ball type), mm	0.2 – 5

Table 1: Characteristics of contact adhesion meter

2.2 Reciprocating Precision Tribometer

We developed a special tribometer with a precision reciprocating motion [6, 7]. It has a controlled normal load of 10 mN – 1 N and sliding velocity of 0.1 – 10 mm/s. To perform the tribotests we selected a sphere-plane scheme, which allows us to calculate most accurately the contact area and pressure as well as to exclude inevitable influence of indenter and plate slopes on the contact geometry. The ball diameter is chosen within 1 – 5 mm according to the required contact pressure. The coatings are applied to the plate (normally silicon), but they can be applied to the ball for widening the range of friction couples under testing. To provide the efficient monitoring of the specimen surface layers before their irreversible damage in testing the tribometer is equipped with an acoustic emission (AE) recording unit. PC with special software allows us to set up the specimen movement velocity, normal load, and rate of counting and amplitude of AE signals in testing. When testing under high frequency and low amplitude of specimen movement it is possible to investigate the dynamics of fretting-wear. The specimen testing process is fully automatic.

The main schematic of the microtribometer is shown in Figure 3.

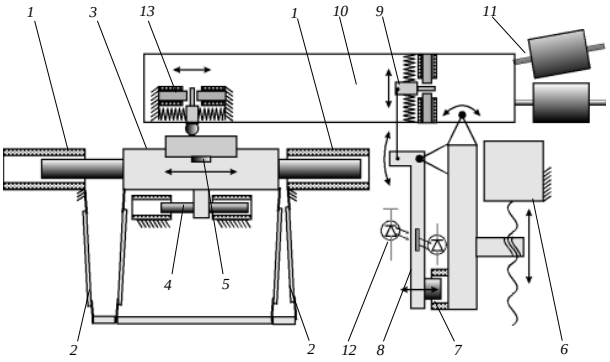

Figure 3: Precision tribometer scheme: 1 — drive electromagnets; 2 — flexible guides; 3 — holder table for specimens; 4 — position transducer; 5 — acoustic emission transducer; 6 — stepping drive; 7 — electromagnet of loading unit; 8 — lever; 9 — loading transducer; 10 — head; 11 — balancing weights; 12 — optocoupler; 13 — friction force transducer

The holder of the plate specimen 3 is connected to the anchors of drive electromagnets 1 and in testing it reciprocates in the horizontal plane. A system of levers and springs that form an elastic suspension is used as movement guides. Usage of flexible guides 2 allows us

to avoid the occurrence of such negative factors as jumpwise displacement at low sliding velocities as well as noise and vibration being characteristic of traditionally used sliding and rolling guides. Owing to the symmetrical design of the guides the normal displacement of the specimen is absent during the holder movement.

Usage of the contactless drive is minimizing the mechanical noise and vibration that negatively affected the measurement of low friction forces. The electromagnetic drive in combination with the flexible guides makes possible to move specimens within the required velocity range with a stroke length from 0.1 to 10 mm. In addition, the electromagnetic drive is helpful in realization of different modes of specimen movement.

It is known that the validity of the tribotest results is directly related to the stiffness of displacement control and friction force measuring system. Regardless the drive design for moving the specimens (piezoelectric or electromagnet) the occurrence of the friction force in ball-plate interaction influences the uniformity of the drive movement, which results in errors in the friction force measurement. In case of including displacement transducers 4 into the feedback system the influence of the friction force on the drive movement parameters can be partially compensated. It is found experimentally that the use of feedback by the specimen position results in drive stiffness increase by an order of magnitude and even more at invariable parameters of the electromagnets and suspension rigidity. A contactless unit consisting of two coils fixed to the stationary base and a moving core mechanically attached to the drive elements is used as a transducer of the specimen holder position. The coil windings are included into the half-bridge scheme that records the core position changing the coil inductance. The given scheme for measuring displacements is less subjected to the influence of environment in contrast to the capacity measurement systems used in SFA [4]. The disadvantage of the inductance transducers is related to their lower sensitivity compared to capacity ones as well as undesirable influence of the alternating magnetic field excited in the coils on the measurement data.

The normal load of the indenter on the specimen is set and kept constant in testing by an electromagnetic unit with feedback. The traction force of electromagnet *7* (Figure 3) is transmitted with lever *8* through the load transducer *9* to oscillating head *10*. The initial balancing of the head is made with weights *11*. Angular position of the head is monitored with optic couple *12* whose signal depends on the slope angle of lever *8*. Electromagnet *7* and load transducer *9* form a circuit with feedback owing to which the normal load is kept constant regardless the normal displacement of the head due to errors in producing and setting the specimen. Stepping drive *6* is used for moving the indenter to the specimen surface as well as its separation from the surface after testing.

2.3 Rotary/Reciprocating Microtribometer

The scheme of rotary/reciprocating microtribometer is presented in Figure 4.

The base plate 1 is used for support of the tester parts and electric boards with power supply unit. The string suspension 8 supports the loading system. The laser system 9 is used for measuring angle position of the loading system, which depends on value of friction force. The stage 6 is rotated by low speed revolution motor 4. It can be replaced by a reciprocating stage providing the stroke to 5 mm. The device is equipped by system of horizontal positioning 2 for changing the radius of wear track.

The control electric circuit based on digital signal processor is connected to the PC by COM port. When the normal load is applied to the ball the friction force causes rotation of the loading system suspended by vertical string. The mirror fixed on string suspension reflects the laser beam. The beam spot position is detected by photodetector. The position-sensitive detector and electromagnetic system assembled with string suspension are connected with feedback circuit to compensate the friction force. This system supports the constant angle position of the loading system during the test. PC records the value of current in the winding of electromagnetic system proportional to the value of friction force.

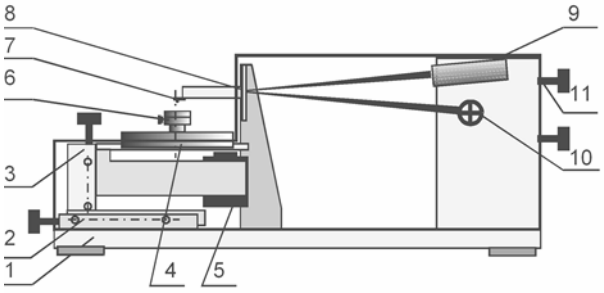

Figure 4: General scheme of rotary/reciprocating microtribometer: 1 – base plate; 2 – horizontal positioning plate; 3 – system of vertical positioning; 4 – rotary or linear electromagnetic motor; 5 – electromagnet; 6 – sample stage; 7 – ball holder; 8 – spring suspension; 9 – laser; 10 – four-quadrant photo detector; 11 – tuning screws.

The loading system consists of permanent magnet, steel ring, winding, holder of ball specimen and balancing weight. The loading force is caused by the interaction between electrical current passed through the winding and magnetic field of the permanent magnet. The magnitude of produced force is independent from the angular position of the holder. It means that the magnitude of load applied by the loading system is independent from the topography effect and small tilt angles of the specimen. Technical specification of the rotary/reciprocating microtribometer is listed in the Table 2.

Normal load, mN	0.01 – 10
Sliding speed, mm/s	0.06 - 4
Radius of wear track, mm	to 10
Ball size, mm	0.2 – 4

Table 2: Characteristics of rotary/reciprocating tribometer

3 TEST SAMPLES

We measured the adhesion and friction forces of thin coatrings and different self-assembled monolayers, which are used in microsystems. Organic SAMs were DDPO4 (dodecylphosphoric acid ester) and ODPO4 (octadecylphosphoric acid ester). Chemical structure and method of deposition is described elsewhere [8]. For DDPO4 and ODPO4 SAMs the initial silicon substrates were covered by Ti or TiOx sublayers. Polymer SAMs were OTS (octadecyltrichlorosilane), SEBS (saturated styrenic thermoplastic elastomer) and Epoxilane. Deposition method of polymer SAM can be found elsewhere [9, 10, and 11]. Polymer SAMs were deposited on silicon substrates. Also substrates of SAMs and thin DLC coating on silicon substrate were tested. Basic characteristics of the specimens being tested are listed in Table 3.

Sample	Description
Si	Substrate
Ti	Ti coating (100 nm) on Si substrate
TiO_x	TiOx coating (20 nm) on Si substrate
DLC	Diamond like carbon (~200 nm) on Si substrate
Ti-$ODPO_4$	Octadecylphosphoric acid ester (2.2 nm) on Ti covered Si substrate
TiOx-$ODPO_4$	Octadecylphosphoric acid ester on TiOx covered Si substrate
TiOx-$DDPO_4$	dodecylphosphoric acid ester on TiOx covered Si substrate
OTS	Octadecyltrichlorsilane (2.6 nm) on Si substrate
SEBS	Poly[styrene – b - (ethylene-co-butylene) - b- styrene] (1.67 nm) on Si substrate
Epoxilane	SAM (~1 nm) with epoxy surface groups on Si substrate

Table 3: Basic characteristics of the specimens

All tests were carried out at a temperature 18±2°C, atmospheric pressure 740±15 mm Hg and relative humidity 60-70%.

4 TEST RESULTS AND DISCUSSION

4.1 Measurement of adhesion

Typical dependence of adhesion force during approaching of various balls to the investigated samples obtained by developed contact adhesion meter is shown on the Figure 5. It shows three experimental dependences of force interaction on the distance obtained with different probes and samples. The curves are obtained in approaching of solids. They illustrate the kinetics of force interaction between the contact surfaces.

We used two spherical indenters as the test counterbodies: a silicon ball (diameter 2 mm), titanium ball (diameter 3 mm).

Curve 1 corresponds to interaction between the silicon ball and the silicon substrate coated with TiO_x on which a monomolecular layer of $ODPO_4$ is deposited. Curve 2 describes interaction between the titanium ball and the silicon plate.

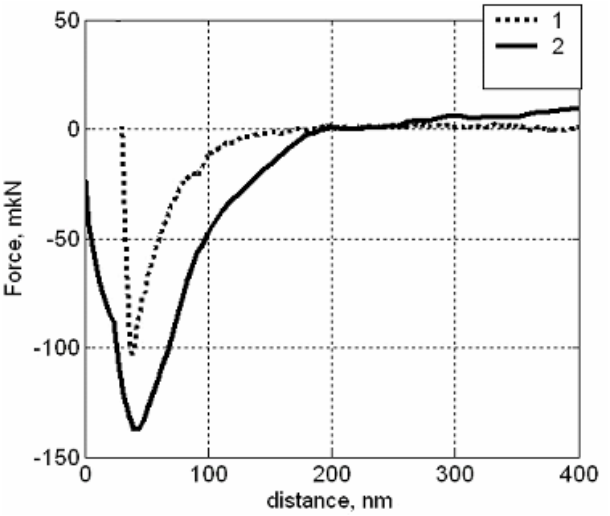

Figure 5: Experimental dependence force - distance. 1 – interaction of silicon ball and Si+TiOx+ODPO4. 2 – interaction between titanium ball and silicon plate.

Pattern of experimental data shows that irrespective of the nature and structure of contacting solids the force-distance curves have similar shapes. Starting from some distance the attraction force between solids monotonously grows up, then the direction of the force reverses. At this stage attraction stops to dominate and the phenomenon of repulsion occurs which grows much faster in comparison with attraction.

Figure 6 shows measurements of distance where attraction begins (radius of force field action) and the maximal force of attraction between solids.

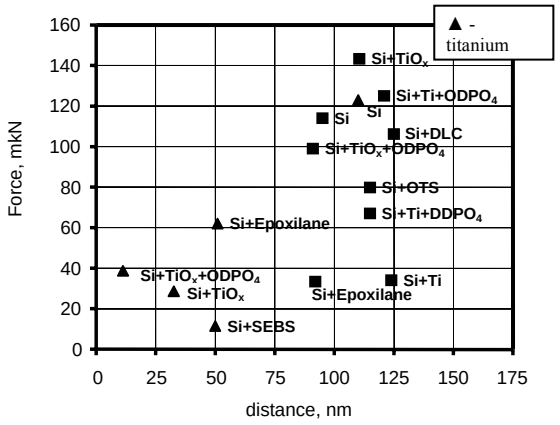

Figure 6: Test values of action radius of attraction force and magnitude of the maximal attraction force for various indenters

From Figure 6 it is clear that the obtained results can be broken into two groups. One group is the results obtained with the use of a silicon probe and coatings. Values of distances of interaction between silicon ball and test sample lay in a range from 90 nm (silicon - $Si+TiO_x+ODPO_4$) up to 125 nm (silicon - DLC).

The second group of data is formed by measurements with titanium ball as a probe. Values of interaction distances lay in a range from 14 nm ($Si+TiO_x+ODPO_4$) up to 50 nm ($Si+TiO_x+ODPO_4$).

Exception is a point relating to interaction between titanium ball and silicon plate (110 nm) being quite close to the point obtained for silicon ball interaction with Ti coating. This fact can be an additional confirmation of the technique reliability.

For calculation of specific surface energy γ of samples it is necessary to know the same characteristic for probes. For a silicon ball it can be obtained from experimental data of interaction with a silicon plate. We found specific surface energy of silicon applying well-known equation of point contact with adhesion interaction $P_{max}=2\pi R(\gamma_{probe}+\gamma_{sample})$. Measuring the force P_{max}, at which two identical bodies are in a point contact, it is possible to calculate their specific surface energy. We calculated the specific surface energy of silicon to be equal 0.0091 J/m^2.

Calculation of specific surface energy of tested samples was carried out at known specific surface energy of a silicon ball. The maximal force of attraction P_{max} and distance of attraction were determined from experimental data (Table 5). The table also includes calculated specific surface energy of tested samples. Calculated values γ for samples Si and Si+Epoxilane are very close to values, which are obtained at interaction of these samples with silicon ball. In contrary to these results, values γ for coatings $Si+TiO_x+ODPO_4$ and $Si+TiO_x$ are much different.

In Figure 7 we present the forces normalized by radius of indenter for contact adhesion meter (CAM) in comparison with the similar data obtained with AFM [12]. The data well concise except with AFM pull-off force measurements on Ti and TiO_x samples. For our opinion the difference can be explained by influence of capillary forces and low hydrophobic properties of the samples. For the much bigger size of indenter of adhesion meter comparing to AFM tip, capillary forces should play dominant role in the interaction of samples during retraction.

Another reason of difference in measurement data for CAM and AFM can be related to different kinematics of the instruments. In case of AFM we have a dynamic system while in CAM case it is quasi-static one. Obviously, both have certain advantages and disadvantages depending on the type of the experiment. In case of CAM the advantage compare to AFM is the absence of jump-like motion of the probe at a small distance from the sample. That gives the possibility to record the force-distance curve completely.

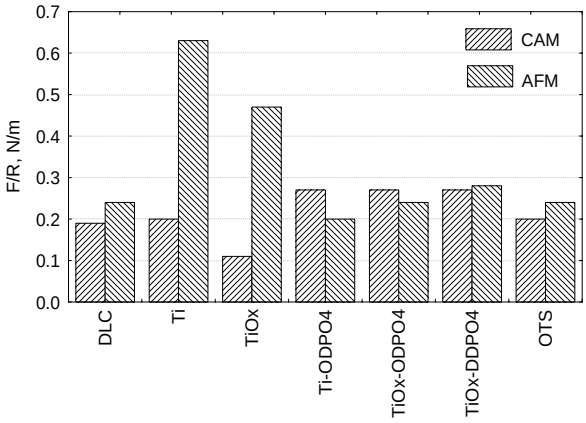

Figure 7: Adhesion (CAM) and pull-of forces (AFM) of the specimens.

Specimens	Attraction force P_{max}, $N*10^{-6}$	Distance of attraction h, $m*10^{-9}$	Specific surface energy γ, J/m^2
Test solid – silicon, radius of $1*10^{-3}$ m			
Si	114	95	0.009
Si+Ti	34	124	0.004
$Si+TiO_x$	143	111	0.014
$Si+TiO_x+ODPO_4$	99	91	0.007
$Si+Ti+ODPO_4$	125	121	0.011
$Si+Ti+DDPO_4$	67	115	0.002
Si+DLC	106	125	0.008
Si+epoxilane	33	92	0.004
Si+OTS	80	115	0.004
Test solid – titanium, radius of $1.5*10^{-3}$ m			
Si	123	110	0.009
Si+epoxilane	38	51	0.003
Si+SEBS	12	50	0.002
$Si+TiO_x+ODPO_4$	34	14	0.004
$Si+TiO_x$	28	33	0.002

Table 5: Experimental and calculated characteristics of tested materials

4.2 Measurement of friction

Experimental tests with reciprocating microtribometer were done with 3mm diameter steel ball and DLC coating on a silicon substrate. The result of tests for normal load of 0.2 mN (gray line) and 0.5 mN (black one) at sliding speed of 0.1 mm/s are given in Figure 8. We can see the instability of data at lower load which is in the range of the action of surface forces – adhesion, capillary forces, and possible electrostatic and magnetic effects.

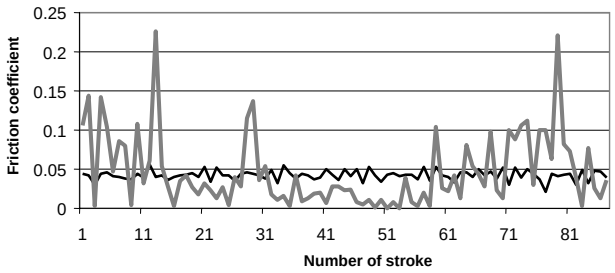

Figure 8: Friction coefficient measured for the same conditions and test samples at various loads close to the range of adhesion forces

Taking in mind the complexity of friction force measurement at very light loads we made the tests in the load range of dozens of mN with precision reciprocating tribometer having a stabilized motion control.

Figure 8 shows the test results of the monomolecular coating SEBS deposited to the silicon substrate. A ball 3 mm in diameter made of steel 52100 **(AISI)** was used as a counterbody.

Simultaneously with the recording of the friction force the rate of counting AE pulses is recorded from the transducer output that is located under the plate specimen. It is seen that the rate of AE counting provides an additional information on friction behavior of the system.

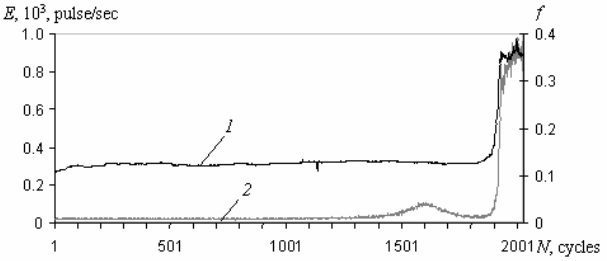

Figure 8: Friction coefficient f (1) and AE counting rate E (2) vs. number of test cycles N. Normal load P = 300 mN; sliding velocity v = 4 mm/s, track length S = 3 mm

Table 6 presents data on friction coefficient of the investigated samples obtained with load 10 mN and sliding speed 0.5 mm/s.

Coating	Thickness, nm	Friction coefficient	Number of cycles
Si	1.2	0.12	20 000
$DDPO_4$	1.67	0.08	250
$ODPO_4$	2.2	0.09	350
OTS	2.6	0.08	20 000
SEBS	8	0.09	20 000

Table 6: Friction coefficients for test samples

5 CONCLUSIONS

The progress in analytical tools as STM, AFM, micro/nanohardhess testers is not adequate for solution of engineering problems arising in microsystems because most of the tools have contact geometry different of real components. Some of these instruments operate in dynamic conditions and this fact should be taken into account when interpreting the data.

The contact adhesion meter having a quasi-static design can provide valuable data on force-distance behavior of solids at nanoscale distances. These data can be efficiently used in addition to AFM and SFA data.

The investigation of friction characteristics of miniature components, thin films and coatings makes necessary some special testing conditions such as light normal loads, low sliding velocity and high sensitivity of friction force measuring systems. It is also important that mechanical noise of the motor system must be limited especially in case of acoustic or electrical measurements combined with tribotesting. But in some cases the decreasing the normal load to the limits where it is comparable with the surface forces makes the tribotest data unreliable.

The work was partially supported by the SCOPES grant 7BYPJ065579 and the grant INTAS 99-0671.

6 REFERENCES

[1] Handbook of Micro/Nano Tribology. ed. Bh. Bhushan, CRC Press, New York, 1995

[2] Sitti, M., Horiguchi, S., Hashimoto, H.: Tele-touch feed-back of surfaces at the micro/nano scale. Proc of IEEE/RSI Int. Conf. on Intelligent Robots and System, 1999, Korea

[3] Israelachvili, J. N.: Adhesion, Friction and Lubrication of Molecularly Smooth Surfaces. In: Fundamentals of Friction: Macroscopic and Microscopic Process. ed. I.L. Singer, H.M. Pollock, Kluver Acad. Pub., London, 1991, 351-385

[4] J.N. Israelachvili: Intermolecular and Surface Forces, NY, 1991

[5] Deryagin, B.V., Krotova, N.A., Smilga, V.P.: Adhesion of Solids. Ed. Nauka, Moscow, 1973

[6] Myshkin N.K. et al.: 47th Int. Sci. Coll., Tech. Univ., 2002, Ilmenau.

[7] Myshkin N.K., et al.: 14th Int. Coll. Tribology, 2004, Esslingen.

[8] Hofer R., Textor M., Spencer N.D.: Alkyl Phosphate Monolayers, Self-Assembled from Aqueous Solution onto Metal Oxide Surfaces. Langmuir, 17 (2001), 4014-4020

[9] Tsukruk V. V., Luzinov I., Julthongpiput D.: Sticky Molecular Surfaces: Epoxysilane Self-Assembled Monolayers. Langmuir, 15 (1999), 3029

[10] Luzinov D., Julthongpiput D., Tsukruk V. V.: Thermoplastic Elastomer Monolayers Grafted to a Silicon Substrate. Macromolecules, 33 (2000), 7629

[11] Julthongpiput D., Ahn H.-S., Sidorenko A., Kim D.-I., Tsukruk V.V.: Towards Self-Lubricated Nanocoatings. Tribology Int., 35 (2002), 829-836

[12] Myshkin, N.K. at al: Smart Surfaces in Tribology: Advanced Additives and Structured Coatings, 2003, Zurich, Switzerland